Available online at www.sciencedirect.com
ScienceDirect
Chemical Geology 247 (2008) 100–118
CHEMICAL GEOLOGY INCLUDING ISOTOPE GEOSCIENCE
www.elsevier.com/locate/chemgeo

Simultaneous determinations of U–Pb age, Hf isotopes and trace element compositions of zircon by excimer laser-ablation quadrupole and multiple-collector ICP-MS

Hong-Lin Yuan [a,b,*], Shan Gao [a,b], Meng-Ning Dai [a], Chun-Lei Zong [a], Detlef Günther [c], Gisela Helene Fontaine [c], Xiao-Ming Liu [a], ChunRong Diwu [a]

[a] State Key Laboratory of Continental Dynamics, Department of Geology, Northwest University, Xi'an, 710069, China
[b] State Key Laboratory of Geological Processes and Mineral Resources, Faculty of Earth Sciences, China University of Geosciences, 430074, China
[c] Laboratory of Inorganic Chemistry, ETH Zurich, 8093 Zurich, Switzerland

Received 11 April 2007; received in revised form 8 October 2007; accepted 9 October 2007

Editor: R.L. Rudnick

Abstract

We describe an *in situ* method for simultaneous measurement of U–Pb–Hf isotopes and trace element compositions of zircons using a quadrupole and multiple-collector inductively-coupled-plasma mass spectrometer (Q-ICP-MS and MC-ICP-MS, respectively) connected to a single excimer laser-ablation system. A laser-generated zircon aerosol was split behind the ablation cell into two transport tubes via a Y-shaped connector and simultaneously introduced into the two mass spectrometers. Hafnium isotopes were measured on the MC-ICP-MS instrument, while U–Pb ages and trace element compositions were determined using the Q-ICP-MS. The precision and accuracy of this method was evaluated using six well-known and widely used zircon standards (91500, Temora-2, GJ-1, Mud Tank, BR266 and Monastery). Analyses were carried out using spot sizes of 32, 44 and 60 μm. For the 44 and 60 μm spot, the resulting U–Pb ages, Hf isotopic and rare earth element (REE) compositions of these six zircons agree with recommended/reported values within 2σ error. The difference in relative standard deviations (RSD) of $^{206}Pb/^{238}U$ ages between split-flow measurements and those obtained separately on the Q-ICP-MS is within ~20% for 91500, Temora-2 and GJ-1, and ~60% for Mud Tank (due to its lower U and Pb concentrations). Our method provides a precise approach for determining the U–Pb age and the Hf isotopic and trace element compositions of zircon within a single ablation event. This is in particular important for analysis of zircons that are small or contain complicated zoning patterns. Finally, the REE composition of zircon BR266 is more homogeneous than other zircons and could be a suitable standard by which to benchmark new standards for microprobe analyses of zircons.

Keywords: Zircon; Hf isotopes; U–Pb dating; Trace elements; Laser ablation; ICP-MS

1. Introduction

Zircon ($ZrSiO_4$) is one of the most widely used accessory minerals in determining the age, origin, and

* Corresponding author. State Key Laboratory of Continental Dynamics, Department of Geology, Northwest University, Xi'an, 710069, China. Tel.: +86 29 88305924; fax: +86 29 88303447.
E-mail address: hlyuan@263.net (H.-L. Yuan).

0009-2541/$ - see front matter © 2007 Elsevier B.V. All rights reserved.
doi:10.1016/j.chemgeo.2007.10.003

thermal history of rocks and deciphering the evolution of the crust and mantle of the Earth in terms of U–Th–Pb–Hf–O isotopic systematics and trace element compositions. The utility of zircon is mainly due to its high closure temperature, resistance to late disturbance, and high concentrations of the parent element uranium, daughter element hafnium, and rare earth elements (REE), especially heavy rare earth elements (HREE), coupled with an extremely low Lu/Hf ratio and negligible incorporation of the daughter element lead and parent element lutetium during crystallization. In addition, two geochronometers ($^{235}U-^{207}Pb$ and $^{238}U-^{206}Pb$) can be used to test the concordance of the determined age (Patchett et al., 1981; Kinny and Maas, 2003; Harrison et al., 2005; Hawkesworth and Kemp, 2006a).

The zircon thermometer also provides important information on the formation and evolution of the continental crust (Watson and Harrison, 2005; Watson et al., 2006). Prior to 1995, Hf isotopic compositions were generally measured by thermal-ionization mass spectrometry (TIMS), but multiple-collector inductively-coupled-plasma mass spectrometry (MC-ICP-MS) (Walder et al., 1993; Halliday et al., 1998; Albarède et al., 2004) has become a powerful alternative method in recent years. The ICP-based technique provides a high-temperature plasma source that ionizes elements with high first-ionization potentials, such as hafnium. The number of studies undertaken using the Lu–Hf isotopic system has increased dramatically with the advent of the MC-ICP-MS technique, although the mass bias of this approach is about 10 times greater than that typically measured by TIMS.

It is therefore necessary to characterize the mass bias in greater detail, especially for those cases in which isobaric interference corrections are applied (Chu et al., 2002; Vance and Thirlwall, 2002). It has been suggested that mass bias in MC-ICP-MS can be corrected using elements with comparable masses to the element of interest (e.g., Zn for Cu, Tl for Pb) (Longerich et al., 1987; Maréchal et al., 1999; Kamenov et al., 2004; Wu et al., 2006a).

The exceptional ionization efficiency of the plasma source, easy sample handling, and absence of polyatomic interference makes MC-ICP-MS the preferred technique for Lu–Hf isotope analyses of zircon (Andersen et al., 2002; Griffin et al., 2002; Woodhead et al., 2004). Indeed, the importance of the Lu–Hf isotopic system in zircon, as measured by MC-ICP-MS, is widely accepted (Blichert-Toft and Albarède, 1997; Blichert-Toft et al., 1999; Zheng et al., 2005; Wu et al., 2006b).

Zircon grains commonly exhibit a complicated growth zonation, particularly in metamorphic rocks. In such cases, *in situ* microanalysis, cathodoluminescence (CL) images, and backscattered electron (BSE) images are required for accurate interpretations of the geological significance of multiple zircon ages (Hoskin and Schaltegger, 2003). Therefore, the simultaneous *in situ* analysis of U–Pb isotopes, Hf isotopes, and trace elements is important in determining zircon geochronology and interpreting geological ages. Although large-geometry SIMS instruments (e.g., the sensitive high-resolution ion microprobe, or SHRIMP) are powerful in this regard, this approach is hampered by the following shortcomings: limited access to instrumentation, sensitivity to the so-called matrix effects, and failure to analyze Hf isotopes. Recent improvements in instrumentation and methodology show that laser-ablation-inductively-coupled-plasma mass spectrometry (including quadrupole and multiple collector, abbreviated as LA-Q-ICP-MS and LA-MC-ICP-MS) has become a powerful tool, providing age dates and trace element concentrations comparable to those of SIMS in terms of both accuracy and precision (Horn et al., 2000; Ballard et al., 2001; Li et al., 2000, 2001; Belousova et al., 2002; Košler et al., 2002; Jackson et al., 2004; Yuan et al., 2004; Paul et al., 2005; Simonetti et al., 2005). More importantly, LA-MC-ICP-MS is currently the only method that can be used to determine *in situ* Hf isotopic compositions (Griffin et al., 2000; Woodhead et al., 2004; Woodhead and Hergt, 2005; Hawkesworth and Kemp, 2006a,b; Wu et al., 2006a).

Previous *in situ* determinations of zircon U–Pb ages and trace element and Hf isotopic compositions using LA-Q-ICP-MS and LA-MC-ICP-MS have been carried out either on different domains of single zircons [e.g., ablation spots for Hf isotopic analyses have been placed close to the spots used for age dating and trace element analysis (Griffin et al., 2000)], on a similar location with different cycles [e.g., one cycle for standard hafnium analysis and a second cycle for measurements of lead isotopes (Woodhead et al., 2004)], or on similar spot locations but with different spot sizes [e.g., a small crater for U–Pb dating and a larger crater on similar locations for Lu–Hf isotope analyses (Wu et al., 2006b)]. In any case, the data are not generated from a single sampling site during a single laser-ablation analysis.

Because zircon is commonly zoned in terms of age and composition, analyses obtained using the above methods represent best estimates, and may or may not be exactly correlative. Woodhead et al. (2004) simultaneously determined $^{207}Pb/^{206}Pb$ ages and Hf isotope data for zircon from a single ablation using an excimer laser-ablation MC-ICP-MS (Nu Plasma) configuration. The authors suggested that the relatively small amount of sample consumed by the SIMS technique means that

it is better to first date zircon by SIMS and then ablate the same domain for Hf isotopes.

In the present paper, we report on the simultaneous *in situ* determination of U–Pb age, Hf isotopes, and trace element compositions from a single laser spot in zircon, accomplished by connecting Q-ICP-MS and MC-ICP-MS to an excimer laser-ablation system. The laser aerosol split-flow system was optimized and studied in terms of precision and accuracy using six well-known and well-characterized zircon standards.

2. Instrumentation

The instruments used in this work were a Nu Plasma HR MC-ICP-MS (Nu Instruments Ltd., UK), an Elan 6100 DRC (Dynamic Reaction Cell) Q-ICP-MS (Perkin Elmer/SCIEX, Canada), and a GeoLas 2005 excimer ArF laser-ablation system (MicroLas™ Beam Delivery Systems, Lambda Physik AG, Germany), all housed at the State Key Laboratory of Continental Dynamics, Northwest University, Xi'an, China. The Nu Plasma HR MC-ICP-MS is a second-generation double-focusing MC-ICP-MS with three ion counters and twelve faraday cups. A unique feature of this instrument is a specially designed zoom lens composed of a pair of quadrupole lenses (Belshaw et al., 1998). An Edwards E2M80 source rotary pump was applied in the interface region to improve sensitivity. The detector arrangements and instrument parameters are summarized in Tables 1 and 2, respectively.

The GeoLas 2005 laser-ablation system consists of a COMPexPro 102 ArF excimer laser (wavelength of 193 nm, maximum energy of 200 mJ, and maximum pulse rate of 20 Hz) and a GeoLas 2005 PLUS package (including a laser-beam homogenizing system, a motorized sampling stage, and a viewing system coupled with an Olympus microscope and color CCD). Although the energy density measured in the ablation site may be higher than 45 J/cm^2 for spot sizes of 4–120 μm, it can be flexibly tuned by changing the discharge voltage. A lower energy density can be achieved with the use of an attenuator located at the entrance of the beam delivery system. The energy density used in this study was 15–20 J/cm^2. Although laser-ablation systems with other wavelengths (i.e., 266 and 213 nm) have also been widely applied, the 193 nm excimer laser-ablation system has been demonstrated to yield superior control in ablation and smaller particle sizes, thereby greatly enhancing vaporization, atomization, and ionization within the ICP. Indeed, improved sensitivity and

Table 2
Instrumental parameters of excimer laser-ablation quadrupole and multiple-collector ICP-MS

	MC-ICP-MS	Q-ICP-MS
Instrument model	Nu Plasma	Elan 6100DRC
RF forward power	1300 W	1350 W
Reflected RF power	<10 W	Unavailable
Plasma gas flow rate	13 L/min	13.5 L/min
Auxiliary gas flow rate	0.8 L/min	0.9 L/min
Make up gas flow rate	0.85 L/min	0.82 L/min
Interface cones	Nickel	Nickel
Sensitivity on solution	200 V/ppm on total Hf beam via DSN+Big-80 pump	50 Mcps/ppm on total U signal via PFA microflow nebulizer
Integration time	0.2 s for laser, total time 50 s	0.015 s for ^{206}Pb and ^{207}Pb and 0.01 s for other trace elements, total time 50 s
Background/ baseline	50 s on-peak-zero (OPZ)	50 s

Laser-ablation system (GeoLas 2005)	
Laser system	ComPexPro 102, ArF excimer, wavelength UV 193 nm
Energy	15–20 J/cm^2
Spot size	44 μm for the HfUPbTr method and 32, 44, 60 μm for the other four methods
Pulse rate	10 Hz for the HfUPbTr method and 4–10 Hz for the other four methods
Carrier gas flow rate	0.8–1.0 L/min

Table 1
Nu Plasma U–Pb block assignments for *in situ* hafnium isotopic composition measurement

Detector[a]	Ex-H	H6	H5	H4	H3	H2	H1	Ax	L1	L2	IC0	IC1	L3	IC2	Ex-L
Amu	182	180	179	177	176	175	174	173	172	171	–	–	–	–	–
Isotopes	W	Hf, W	Hf	Hf	Hf, Lu, Yb	Lu	Hf Yb	Yb	Yb	Yb	–	–	–	–	–

Note the gaps in the collector assembly between Ex-H and H6, H5 and H4, and L2 and IC0.
[a] Ex-H, H6 to H1, Ax, L1 to L3 and Ex-L are faraday cups, and IC0 to IC2 are ion counters.

precision, as well as reduced elemental fractionation, have been reported for the 193 mm system (Eggins et al., 1998; Günther and Heinrich, 1999a; Guillong et al., 2003). The laser homogenizer consists of two 13×13 lens arrays, and guarantees cylindrical and flat-bottomed craters on target surfaces. A series of spot sizes (5–200 μm in diameter) are available by switching an aperture located at the end of the laser-beam delivery optics in front of the microscope. In the present study, a spot size of 44 μm was used in developing the method, although spot sizes of 60 and 32 μm were also employed.

Helium was used as a carrier gas to provide efficient aerosol transport to the ICP and minimize aerosol deposition around the ablation site and within the transport tube (Eggins et al., 1998; Günther and Heinrich, 1999b; Jackson et al., 2004). We used high-purity argon (99.9995%) and high-purity helium (99.9995%) purified using an in-house filtration column composed of a 10 L 13× molecular sieve. This column has filtering performance similar to charcoal filters (Hirata and Nesbitt, 1995; Hirata et al., 2005) and gold traps (Storey et al., 2006). Gas purification reduces the gas backgrounds of ^{202}Hg from >800 counts per second (cps) to <200 cps and those of ^{208}Pb from >400 cps to <100 cps. These backgrounds were measured by ion counters (MC-ICP-MS); they correspond to 0.05 and 0.1 parts per trillion (ppt) for ^{202}Hg and ^{208}Pb, respectively.

The Elan 6100 DRC Q-ICP-MS was operated in the normal mode without using the dynamic-reaction cell. The instrument sensitivity was measured to be ~60 million cps for 1 μg/mL of ^{238}U in standard solution nebulization mode [ESI PFA microflow nebulizer (100 μL/min) and cyclonic spray chamber], while the average background intensities were negligible for elements with $m/z \geq 85$ (Rb) (Gao et al., 2002; Yuan et al., 2004). The sensitivity in laser-ablation mode on the NIST SRM 610 was ~2366 cps per μg/g of ^{238}U for Q-ICP-MS (44 μm) and 7–8 V per 1% of hafnium for MC-ICP-MS (44 μm). Count rates for six standard zircons are presented in Table 3.

3. Analytical techniques

3.1. Correction for interference by Lu and Yb

Interference correction for Yb and Lu is of paramount importance for precise *in situ* measurements of Hf isotopes in zircon (Woodhead et al., 2004). Interference by ^{176}Yb is substantial because the Yb content is at least an order of magnitude higher than that of Lu. We were able to use the mass bias from Yb to calculate the mass fractionation of Lu because of the similar physicochemical properties of these HREEs. It has been demonstrated that the mass fractionation of Yb (β_{Yb}) is not constant over time and that β_{Yb} obtained from the introduction of solutions (e.g., doping the JMC 475 Hf solution with varying Yb concentrations) is unsuitable for *in situ* zircon measurements (Woodhead et al., 2004; Iizuka and Hirata, 2005; Wu et al., 2006a).

The U–Pb block detector assembly of the Nu Plasma instrument makes it possible to measure isotopes of 171–177, 179, 180 and 182 atomic mass units (amu) during a single data acquisition. Although the ^{178}Hf signal cannot be acquired, signals were sufficient to obtain precise and geological meaningful ^{176}Hf/^{177}Hf ratios. Among the measured isotopes, the ^{179}Hf/^{177}Hf ratio was applied to calculate the mass fractionation of Hf (β_{Hf}), the ^{175}Lu signal was used to calculate the interference of ^{176}Lu on ^{176}Hf, and ^{173}Yb–^{172}Yb–^{171}Yb was applied to calculate both β_{Yb} and the interference of ^{176}Yb on ^{176}Hf.

The measurements also provided the opportunity to assess possible differences in the β_{Yb} value calculated from ^{173}Yb/^{171}Yb, ^{173}Yb/^{172}Yb, and ^{172}Yb/^{171}Yb (Vervoort et al., 2004). Because of the limited number of partially fixed faraday cups, it has been proposed that either ^{173}Yb/^{171}Yb or ^{173}Yb/^{172}Yb be used as the reference in calculating β_{Yb}. Fig. 1 compares β_{Yb} calculated from the ^{173}Yb/^{171}Yb, ^{173}Yb/^{172}Yb, and ^{172}Yb/^{171}Yb ratios of standard zircons with various Yb concentrations. The obtained ^{176}Hf/^{177}Hf ratios based on the *in situ* β_{Yb} [model 1, the ^{173}Yb/^{171}Yb ratio measured

Table 3
Average intensities of lead and uranium of Q-ICP-MS and hafnium of MC-ICP-MS for simultaneous measurement

	Total radiogenic lead (cps)				Uranium (cps)				Hafnium (V)		
Method	UPb	UPbTr	HfUPb	HfUPbTr	UPb	UPbTr	HfUPb	HfUPbTr	HfUPb	HfUPbTr	Hf
Spot size, μm	32	32	44	44	32	32	44	44	44	44	44
91500	18,339	21,862	29,386	28,964	84,744	102,660	126,955	127,292	4.2	5.2	7.2
Temora-2	11,704	13,252	11,836	8371	142,978	176,708	152,437	111,859	3.7	4.7	6.6
GJ-1	25,638	26,655	30,974	20,963	253,014	257,857	309,673	225,522	4.3	5.8	7.5
BR266	52,205	45,906	110,709	137,369	514,543	416,291	1,104,434	1,396,851	3.9	4.4	7.1
Mud Tank	6990	4540	7053	4738	49,047	30,741	50,755	36,582	4.8	4.1	9.6
Monastery	462	1142	287	687	9126	8720	15,024	8512	7.6	7.9	12.8

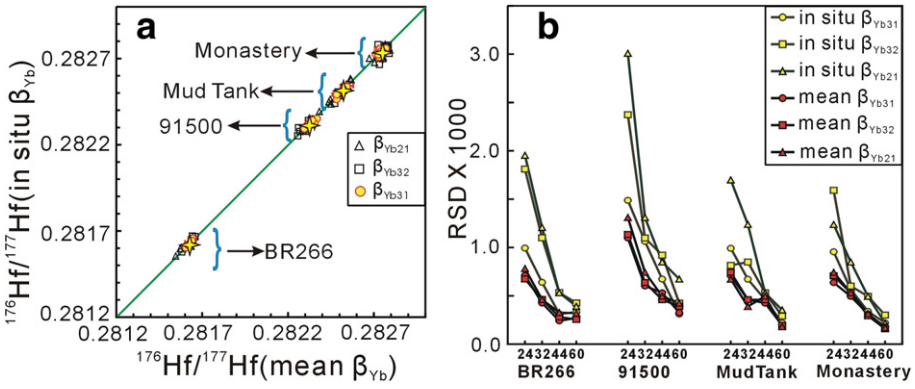

Fig. 1. Comparison of the $^{176}Hf/^{177}Hf$ ratios of four zircon standards (BR266, 91500, Mud Tank, and Monastery) corrected using *in situ* (model 1) and mean β_{Yb} (model 2) values (a) and corresponding relative standard deviations (RSD) (b). Stars in (a) represent recommended $^{176}Hf/^{177}Hf$ ratios (Woodhead and Hergt, 2005; Wu et al., 2006a). For each of the four standards, the RSD in (b) was calculated based on 280 measured $^{176}Hf/^{177}Hf$ ratios from a single run.

on the zircon itself (Woodhead et al., 2004)] corrected for ^{176}Yb interference are consistent with calculations based on the mean β_{Yb} [model 2, the mean $^{173}Yb/^{171}Yb$ ratio (Iizuka and Hirata, 2005) or the mean $^{173}Yb/^{172}Yb$ ratio (Wu et al., 2006a) obtained on the same spot)] corrected for ^{176}Yb interference (Fig. 1a), whereas β_{Yb31} (based on $^{173}Yb/^{171}Yb$) shows the highest accuracy among β_{Yb31}, β_{Yb32} (based on $^{173}Yb/^{172}Yb$), and β_{Yb21} (based on $^{172}Yb/^{171}Yb$). All ^{176}Yb-corrected $^{176}Hf/^{177}Hf$ ratios agree with recommended values within 2σ error (Woodhead and Hergt, 2005; Wu et al., 2006a). The relative standard deviations (RSD) of $^{176}Hf/^{177}Hf$ ratios based on both models are shown in Fig. 1b. The RSDs associated with *in situ* β_{Yb} (model 1) are generally larger than those associated with the mean β_{Yb} (model 2), whereas β_{Yb31} shows lower RSDs than β_{Yb21} and β_{Yb32} for both models (Fig. 1b). Accordingly, the mean β_{Yb31} calculation (model 2) was applied in our analyses. Although similar $^{176}Hf/^{177}Hf$ ratios were obtained on different spot sizes, the RSDs decreased with increasing spot size (Fig. 1b. The RSDs for 44 μm and 60 μm were <0.005%, being similar for each of the four zircons; therefore, a spot size of 44 μm was applied in our analyses unless indicated otherwise. These analyses were then compared to previously reported data generated at spot sizes of 40–94 μm (Griffin et al., 2000; Griffin et al., 2004; Woodhead et al., 2004; Hawkesworth and Kemp, 2006b; Wu et al., 2006a).

3.2. Strategies for simultaneous measurements

Five methods were applied in determining U–Pb–Hf isotopes and trace elements: (1) U–Pb isotopes determined by Q-ICP-MS (herein abbreviated as UPb); (2) U–Pb isotopes and trace elements by Q-ICP-MS (UPbTr); (3) hafnium isotopes by MC-ICP-MS (Hf); (4) hafnium and U–Pb isotopes by the simultaneous use of MC-ICP-MS and Q-ICP-MS (HfUPb); and (5) Hf–U–Pb isotopes and trace elements by the simultaneous use of MC-ICP-MS and Q-ICP-MS (HfUPbTr).

For methods UPb and UPbTr, we used a routine LA-Q-ICP-MS protocol that consisted of 30 s of blank acquisition prior to a 50 s ablation of the zircon (laser frequency, 10 Hz; spot size, 32 μm). For hafnium isotope measurements (Hf), experiments consisted of 50 s of baseline acquisition by the on-peak-zero (OPZ) method, followed by 50 s of zircon ablation (laser frequency, 10 Hz; spot size, 44 μm). For the HfUPb and HfUPbTr methods, the aerosol from a single ablation was transferred from the sample chamber to a Y-shaped glass connector (Fig. 2) via a Tygon tube (inner diameter, 4 mm), where it was split into two transport tubes and simultaneously introduced into both the Elan 6100 DRC (for measurements of U and Pb isotopes and trace elements) and the Nu Plasma (for determination of Hf isotopes). The gas inlet (inner diameter, 4 mm) of the connector was divided centrally, and the two gas outlets (inner diameter, 2 mm) were oriented parallel to each other. The two streams of split aerosol were then separately flushed into homemade homogenizers (Fig. 2d) via tygon tubes of 3 m in length and 2 mm inner diameter. Before entering the plasma, the aerosol was mixed with argon makeup gas in the homogenizers, where adjacent peaks of laser pulses were homogenized.

On the Q-ICP-MS side of this setup, a helium gas [via a mass flow controller (MFC)] was connected to the tube between the Y-shaped splitter and the homogenizer. The flow rates of the helium carrier gas were optimized based on signals on the Q-ICP-MS (~0.5 million cps for ^{238}U of NIST SRM 610, 44 μm), because sensitivities for Q-

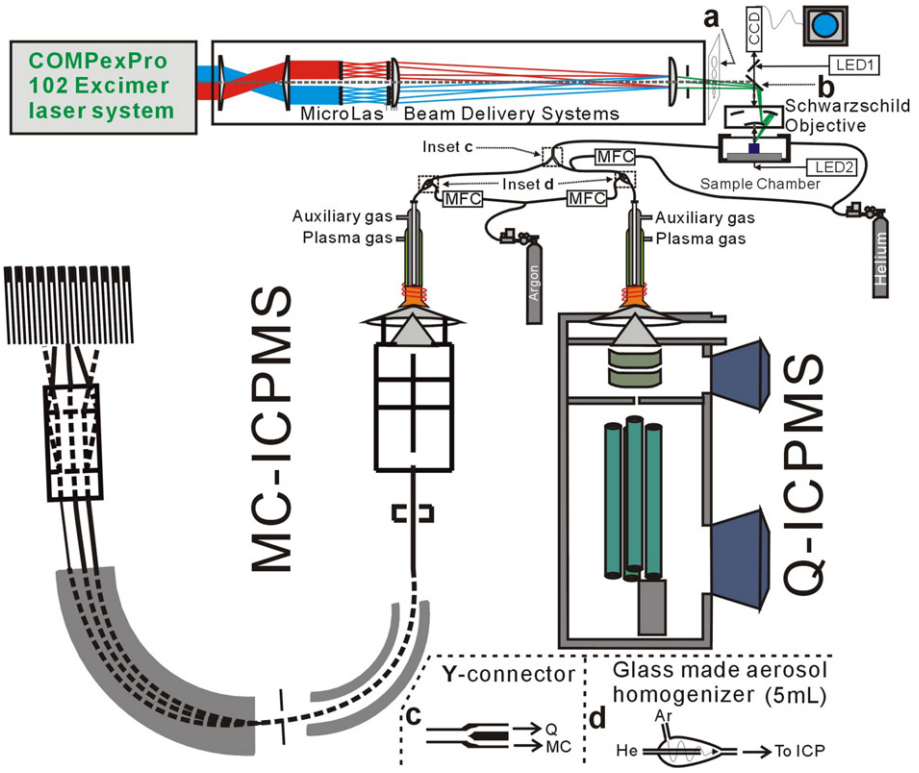

Fig. 2. Schematic diagram of the laser-ablation system setup. The 193 nm laser beam is generated using a COMPexPro 102 ArF Excimer laser, homogenized by a set of beam delivery optics, adjusted in diameter by an aperture (a), deflected by coated deflector mirrors (b), and finally reaches the sample surface by passing through a Schwarzschild objective. The sample is held in a sample chamber, and can be observed under an Olympus optical microscope via a 25× Schwarzschild objective and a CCD monitor. The ablated zircon aerosol carried in helium is split via a Y-shaped connector (c) into two outlet streams that are separately flushed into homemade homogenizers (d) via tygon tubes of 3 m in length and 2 mm inner diameter. The aerosol is mixed with argon makeup gas in the homogenizers. The two streams of aerosol are finally transported into an Elan 6100 DRC Q-ICP-MS (for measurements of U–Pb age and trace element concentrations) and a Nu Plasma HR MC-ICP-MS (for simultaneous hafnium isotope analysis). A mass flow controller (MFC) is connected to the tube between the Y-shaped splitter and homogenizer on the Q-ICPMS side. LED1 and LED 2 indicate reflected and transmitted light.

ICP-MS are generally an order of magnitude lower than those for MC-ICP-MS. Approximately 40% of the aerosol was transferred into the Q-ICP-MS for U–Pb and REE analysis: the remainder was flushed into the MC-ICP-MS for the measurement of hafnium isotopes. Detailed analytical protocols are provided in Table 2.

3.3. Data acquisition

All LA-Q-ICP-MS and LA-MC-ICP-MS measurements were carried out using time resolved analysis (TRA) operated in fast peak-hopping and DUAL detector mode (Q-ICP-MS) using a short integration time. The MC-ICP-MS was operated in static mode. Prior to ablation for U–Pb dating, the zircon was pre-ablated for two laser pulses (UPb, UPbTr, HfUPb, and HfUPbTr) to remove surface contamination (Iizuka and Hirata, 2004). Raw count rates of ^{29}Si, ^{204}Pb, ^{206}Pb, ^{207}Pb, ^{208}Pb, ^{232}Th, and ^{238}U were measured using Q-ICP-MS. Trace elements were also acquired using the UPbTr and HfUPbTr methods. $^{180-179,\ 177-174}$Hf, ^{175}Lu, and $^{173-171}$Yb isotopes were measured by MC-ICP-MS for methods Hf, HfUPb, and HfUPbTr. Concentrations of uranium, thorium, lead, and trace elements were calibrated using ^{29}Si as an internal standard and NIST SRM 610 as the external reference standard. Concentration values of NIST SRM 610 used for external calibration were taken from Pearce et al. (1997). ^{202}Hg was usually <30 cps in the Q-ICP-MS gas blank; therefore, the contribution of ^{204}Hg to ^{204}Pb was negligible, and no correction was applied. ^{207}Pb/^{206}Pb, ^{206}Pb/^{238}U, ^{207}Pb/^{235}U, and ^{208}Pb/^{232}Th ratios were calculated using GLITTER 4.4 (GEMOC, Macquarie University, Sydney, Australia) and corrected for both instrumental mass bias and depth-dependent elemental and isotopic fractionation using zircon 91500 as the external standard. For U–Pb isotope

analyses of zircon 91500, zircon GJ-1 was used as the external standard. Ages were calculated using ISOPLOT (rev. 3) (Ludwig, 2003).

Supplementary Table 1 lists U–Pb data obtained using the four methods with various spot sizes; Supplementary Table 2 lists REE data; and Supplementary Table 3 lists Hf data.

4. Simultaneous measurements of Hf–U–Pb isotopes and trace element compositions of standard zircons

4.1. 91500

Zircon 91500 is one of the most widely applied zircon standards for U–Pb dating and Hf isotopic analysis. This standard is relatively homogeneous in terms of U–Pb isotopic composition, although its overall U and Pb concentrations are low (Wiedenbeck et al., 1995; Košler et al., 2002; Wiedenbeck et al., 2004; Yuan et al., 2004; Wu et al., 2006a). The isotope-dilution thermal-ionization mass spectrometry (ID-TIMS) ages for this zircon are 1062.4±0.8 Ma (2σ) for $^{207}Pb/^{206}Pb$ and 1065.4±0.6 Ma (2σ) for $^{206}Pb/^{238}U$ (Wiedenbeck et al., 1995). Concordia diagram and weighted average $^{206}Pb/^{238}U$ ages for this zircon obtained using our four methods are shown in Fig. 3 [UPb (Fig. 3a,b), UPbTr (Fig. 3c,d), HfUPb (Fig. 3e,f), and HfUPbTr (Fig. 3g,h)]. Both the UPb and UPbTr methods were performed using a spot size of 32 μm. The weighted average $^{206}Pb/^{238}U$ ages obtained using the UPb and UPbTr methods are 1061.8±5.3 Ma [2σ, mean square of weighted deviates (MSWD)=0.13, n=17; Fig. 3b] and 1062.2±6.0 Ma (2σ, MSWD=0.046, n=17; Fig. 3d), respectively. The increased standard error of the UPbTr ages is mainly due to the reduced data-acquisition efficiency for U–Pb isotopes that arises when trace elements are measured in addition to U–Th–Pb (UPbTr method). The weighted average $^{206}Pb/^{238}U$ ages determined using the HfUPb and HfUPbTr methods are 1065.1±3.1 Ma (2σ, MSWD=0.65, n=26; Fig. 3f) for spot sizes varying from 32 to 60 μm and 1063.2±4.4 Ma (2σ, MSWD=0.025, n=21; Fig. 3h) for a spot size of 44 μm.

The ages obtained using all four methods are within 2σ error of the reported ID-TIMS age. The REE concentrations obtained using the UPbTr and HfUPbTr methods are shown in Fig. 4a. The chondrite-normalized REE distributions obtained using both the UPbTr and HfUPbTr methods for various spot sizes overlap with each other and are consistent with recommended values (Whitehouse, 2004; Wiedenbeck et al., 2004; Yuan et al., 2004). The light rare earth element (LREE) contents of zircon 91500 are very low (Fig. 4a). Previous studies revealed that the hafnium isotopic compositions of this standard are heterogeneous, with an essentially bimodal distribution of $^{176}Hf/^{177}Hf$ ratios at 0.282284±0.000022 and 0.282330±0.000029 (2σ) (Griffin et al., 2006). The peaks yield an average value of 0.282307±0.000031 (Wu et al., 2006a).

Fig. 5 compares $^{176}Hf/^{177}Hf$ ratios obtained using the HfUPb and HfUPbTr (Fig. 5a) and Hf (Fig. 5b) methods. The Hf method yielded identical $^{176}Hf/^{177}Hf$ ratios for spot sizes of 32, 44, and 60 μm, which were weighted at 0.282311±0.000005 (2σ, MSWD=0.95, n=31), 0.282305±0.000003 (2σ, MSWD=0.94, n=86), and 0.282310±0.000004 (2σ, MSWD=1.04, n=20), respectively. Combining these data yields a weighted average $^{176}Hf/^{177}Hf$ value of 0.282308±0.000002 (2σ, MSWD=1.00, n=137). Combined data from the HfUPb and HfUPbTr methods for spot sizes of 32, 44, and 60 μm yield weighted average $^{176}Hf/^{177}Hf$ values of 0.282310±0.000022 (2σ, MSWD=0.4, n=12), 0.282309±0.000006 (2σ, MSWD=1.6, n=44), and 0.282310±0.000010 (2σ, MSWD=0.16, n=10), respectively. Taken together, these values give a weighted average $^{176}Hf/^{177}Hf$ ratio of 0.282309±0.000004 (2σ, MSWD=1.12, n=66, spot size=32, 44, and 60 μm). These results agree well with the recommended values (Woodhead et al., 2004; Woodhead and Hergt, 2005; Griffin et al., 2006; Wu et al., 2006a).

4.2. Temora-2

This zircon standard was obtained from the Middledale Gabbroic Diorite, a high-level mafic stock within the Paleozoic Lachlan Orogen of eastern Australia (Black et al., 2004). The standard is coarser grained and more deuterically altered than Temora-1, although both standards have similar ages. The ID-TIMS $^{206}Pb/^{238}U$ age of this zircon is 416.78±0.33 Ma (MSWD=0.56, 95% confidence limits), based on measurement errors alone. Uncertainties related to spike-calibration and the U decay constant limit the accuracy to 416.8±1.3 Ma (Black et al., 2004). The UPb, UPbTr, HfUPb, and HfUPbTr methods yielded weighted average $^{206}Pb/^{238}U$ ages of 415.1±2.1 Ma (2σ, MSWD=0.57, n=19, spot size=32 μm; Fig. 6b), 416.3±3.0 Ma (2σ, MSWD=0.30, n=19, spot size=32 μm; Fig. 6d), 415.3±1.2 Ma (2σ, MSWD=0.72, n=40, spot size=32, 44, and 60 μm; Fig. 6f), and 414.0±2.0 Ma (2σ, MSWD=0.72, n=37, spot size=32, 44, and 60 μm; Fig. 6h), respectively. These ages agree with the ID-TIMS age within 2σ error and are consistent with published LA-Q-ICP-MS ages (Black et al., 2004; Yuan et al., 2004).

The REE concentrations obtained using the UPbTr and HfUPbTr methods are shown in Fig. 4b. Although

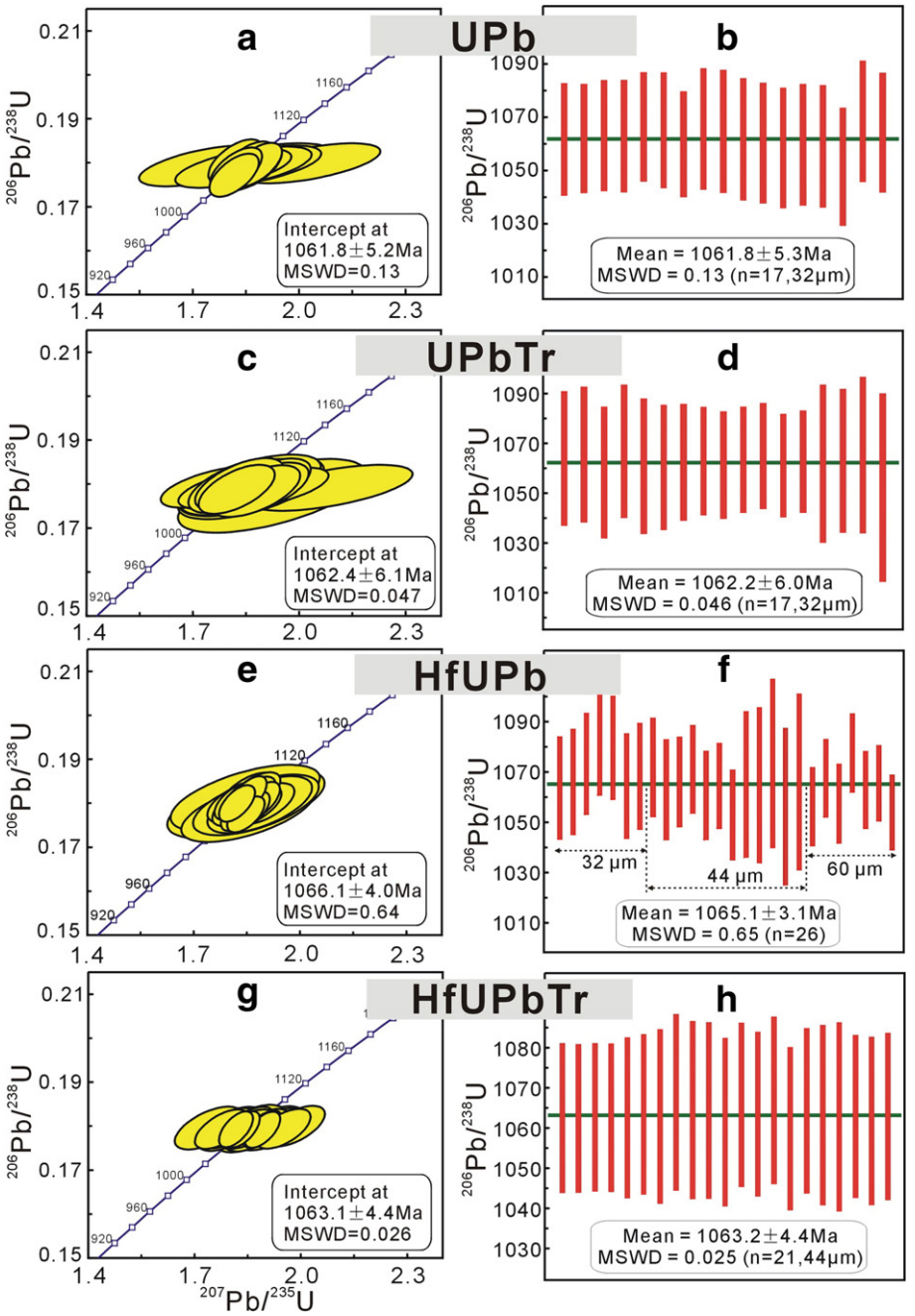

Fig. 3. U–Pb concordia diagrams showing the results obtained for zircon 91500 as measured using (a) the UPb method, (c) the UPbTr method, (e) the HfUPb method, and (g) the HfUPbTr method. Corresponding distributions of the weighted average $^{206}Pb/^{238}U$ ages are shown in (b), (d), (f), and (h), respectively. Uncertainties represent 2σ. MSWD is the mean square of weighted deviates.

the two methods yield overlapping results, consistent with the data reported by Black et al. (2004), the high degree of variation in REE concentrations reveals significant chemical heterogeneity (Fig. 4b). For spot sizes of 32, 44, and 60 μm, the HfUPb and HfUPbTr methods together yield weighted average $^{176}Hf/^{177}Hf$ ratios of 0.282677 ± 0.000010 (2σ, MSWD=0.78, $n=20$), 0.282678 ± 0.000003 (2σ, MSWD=0.68, $n=39$), and 0.282672 ± 0.000009 (2σ, MSWD=2.3, $n=21$), respectively. The Hf method gives 0.282680 ± 0.000005 (2σ, MSWD=2.4, $n=47$) for spot sizes of 32, 44, and 60 μm (Fig. 5d). The overall weighted average of the results

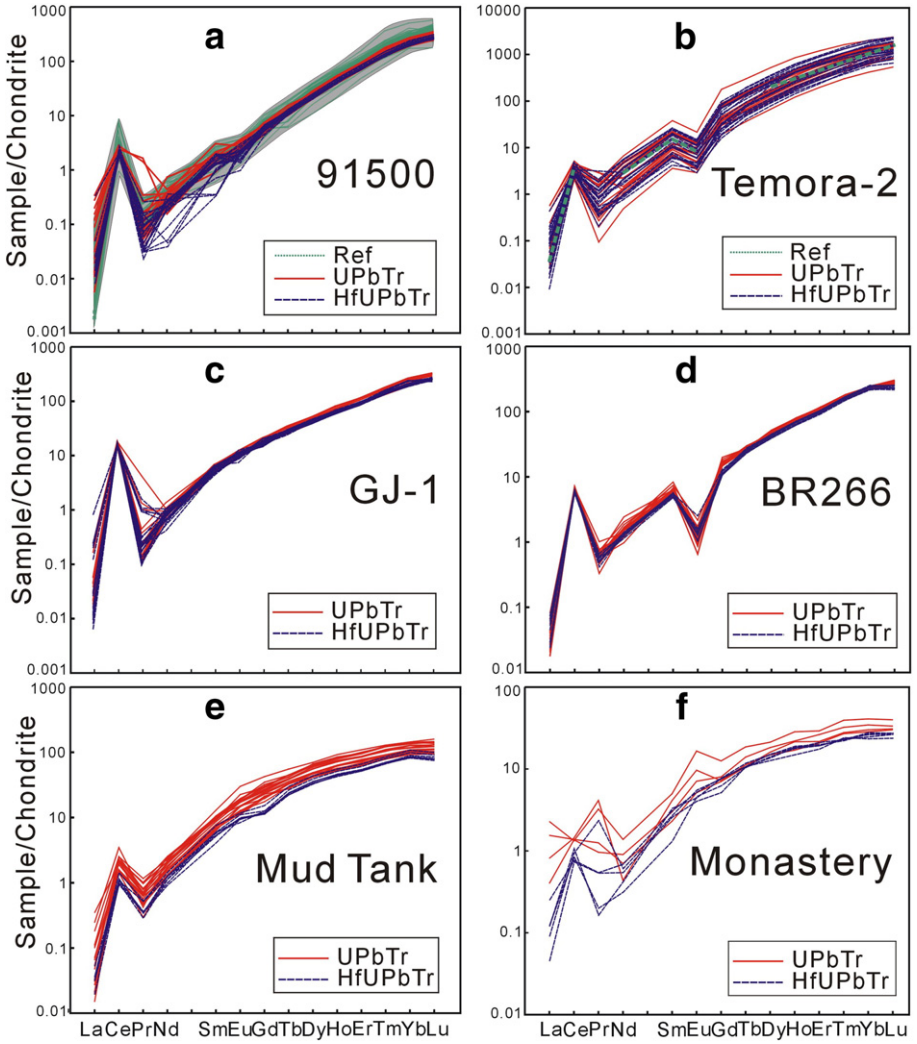

Fig. 4. Chondrite-normalized rare earth element patterns obtained for the six analyzed zircon standards. The grey area represents measurements performed using the UPbTr method on spot sizes varying from 32 to 120 μm. Reference (Ref) values for 91500 are from Whitehouse (2004), Wiedenbeck et al. (2004), and Yuan et al. (2004), while those for Temora-2 are from Black et al. (2004). Chondrite values are from Taylor and McLennan (1985).

obtained using the HfUPb and HfUPbTr methods for the three spot sizes is 0.282677±0.000003 (2σ, MSWD=1.12, n=80; Fig. 5c). These values agree with published results within 2σ error, with the published values ranging from 0.282680±0.000024 (2σ) to 0.282706±0.000020 (2σ) (Woodhead et al., 2004; Xu et al., 2004; Harrison et al., 2005; Qi et al., 2005; Hawkesworth and Kemp, 2006b; Wu et al., 2006a).

4.3. GJ-1

GJ-1 is a colorful, gem-quality zircon (the color varies from red to pinkish-red, yellowish-green, and brown) that is presumably derived from an East African pegmatite (Jackson et al., 2004; Elhlou et al., 2006). The zircon was originally acquired from G&J Gem Merchants (Sydney, Australia) by the GEMOC group (Jackson et al., 2004; Elhlou et al., 2006), who provided the grain analyzed in the present study (1 cm in diameter). ID-TIMS analyses of this zircon yield a highly precise $^{207}Pb/^{206}Pb$ age of 608.5±0.4 Ma and relatively young $^{206}Pb/^{238}U$ age of 599.8±4.5 Ma (mean of the apparent ages) (Jackson et al., 2004).

The results obtained using the UPb, UPbTr, HfUPb, and HfUPbTr methods are shown in Fig. 7. The weighted average $^{206}Pb/^{238}U$ ages obtained using the UPb, UPbTr, HfUPb, and HfUPbTr methods are 604.6±2.9 Ma (2σ, MSWD=0.09, n=19, spot size=32 μm; Fig. 7b), 604.1±3.2 Ma (2σ, MSWD=0.08, n=19, spot size=32 μm; Fig. 7d), 603.5±2.2 Ma (2σ, MSWD=0.38, n=36, spot

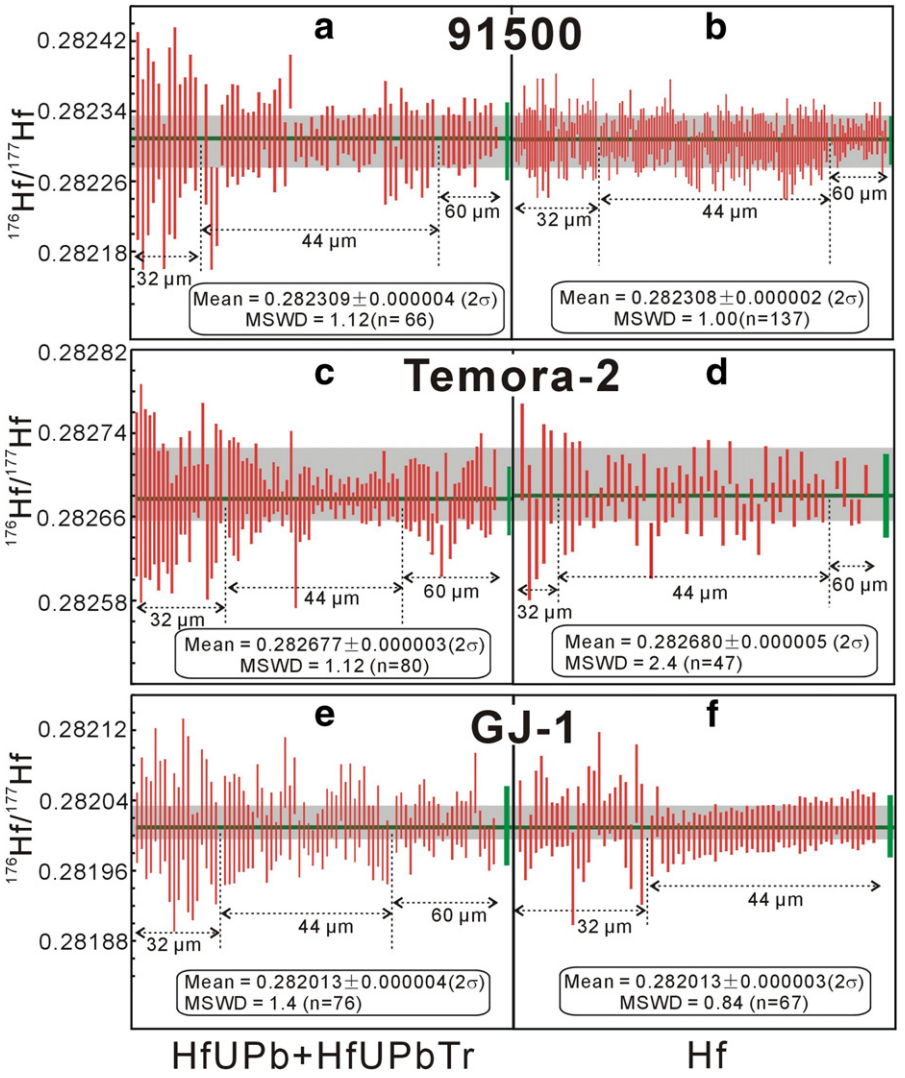

Fig. 5. $^{176}Hf/^{177}Hf$ ratios obtained for zircon standards 91500, Temora-2, and GJ-1. The thick horizontal line and grey area in each panel represent the weighted average $^{176}Hf/^{177}Hf$ ratios from the present study and 2σ error of the recommended values (91500 and Temora-2 from Wu et al., 2006a; GJ-1 from Elhlou et al., 2006), respectively. The thick vertical bar on the right side of each panel represents the 2σ range of the overall weighted average of analyses for spot sizes of 32, 44, and 60 μm.

size=32, 44, and 60 μm; Fig. 7f), and 602.5±2.2 Ma (2σ, MSWD=0.31, n=43, spot size=32, 44, and 60 μm; Fig. 7h), respectively. Some points plot above the concordia curve, probably due to their low ^{207}Pb intensities (629–680 cps), which are difficult to measure precisely (Fig. 7).

Although these ages are slightly younger than the ID-TIMS $^{207}Pb/^{206}Pb$ age, they still agree with the ID-TIMS $^{206}Pb/^{238}U$ age within 2σ error. The REE concentrations measured using the HfUPbTr method overlap with the lower part of the range of results obtained using the UPbTr method. This standard generally shows HREE enrichment and a positive Ce anomaly (Fig. 4c). Hafnium isotopic compositions obtained using the HfUPb+HfUPbTr and Hf methods are shown in Fig. 5e and f, respectively. For a spot size of 32 μm, these values yield weighted average $^{176}Hf/^{177}Hf$ ratios of 0.282013±0.000014 (2σ, MSWD=0.84, n=18) and 0.282015±0.000009 (2σ, MSWD=1.5, n=16), respectively; for a spot size of 44 μm, they yield ratios of 0.282013±0.000008 (2σ, MSWD=1.8, n=36) and 0.282013±0.000004 (2σ, MSWD=0.65, n=51). The overall weighted averages obtained using the HfUPb+HfUPbTr and Hf methods are 0.282013±0.000004 (2σ, MSWD=1.4, n=76, spot

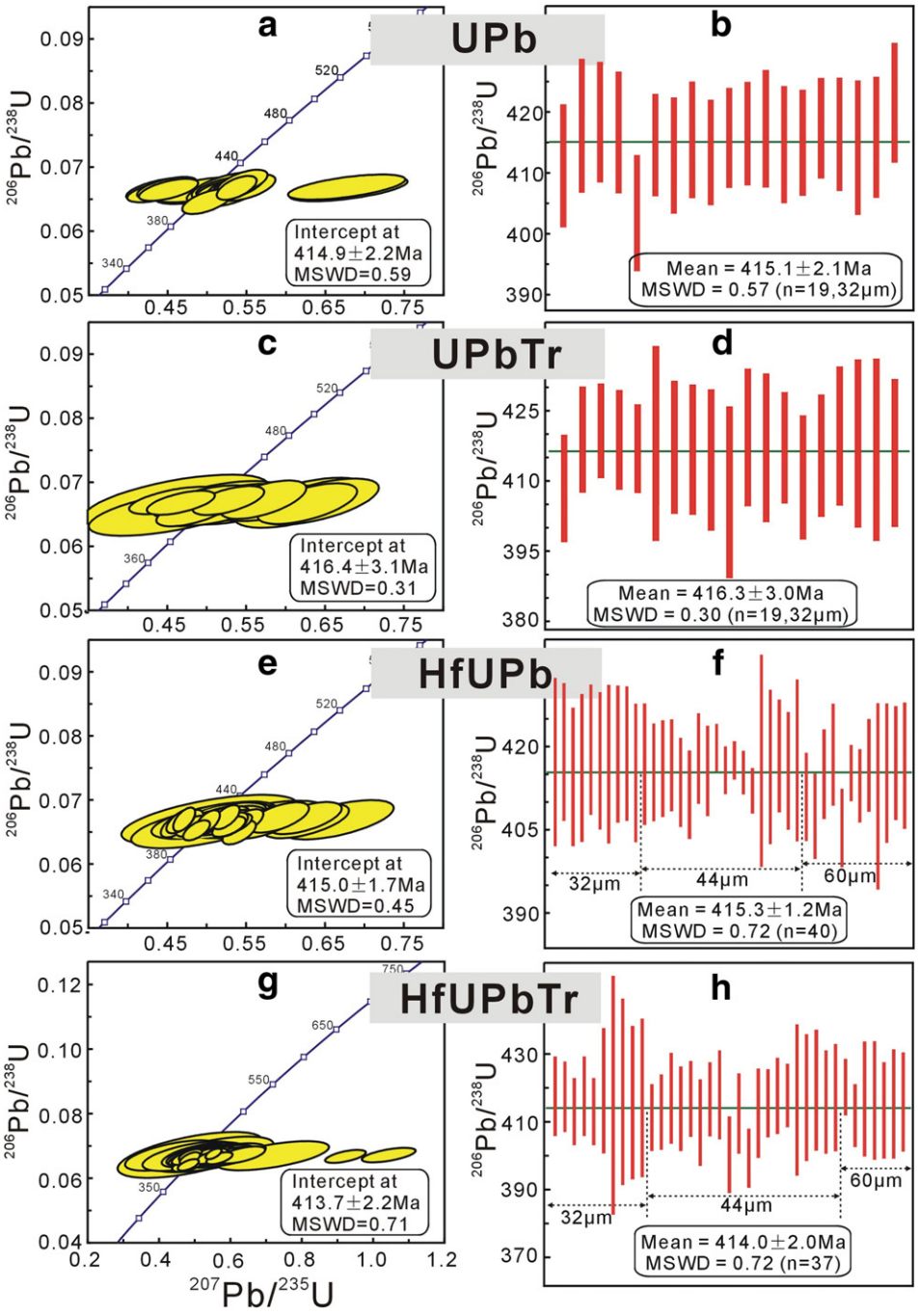

Fig. 6. U–Pb concordia diagrams showing the results obtained for the zircon Temora-2 measured using (a) the UPb method, (c) the UPbTr method, (e) the HfUPb method, and (g) the HfUPbTr method. Corresponding distributions of the weighted average $^{206}Pb/^{238}U$ ages are shown in (b), (d), (f), and (h), respectively. Uncertainties are 2σ.

size=32, 44, and 60 μm; Fig. 5e) and 0.282013±0.000003 (2σ, MSWD=0.84, n=67, spot size=32 and 44 μm; Fig. 5f), respectively. These values agree well with the recommended value of 0.282015±0.000019 (2σ, n=25) reported by Elhlou et al. (2006).

4.4. BR266

BR266 is a Sri Lankan gem-quality zircon that has been used as an ion microprobe reference material by the Geological Survey of Canada (Stern, 2001). The ID-TIMS

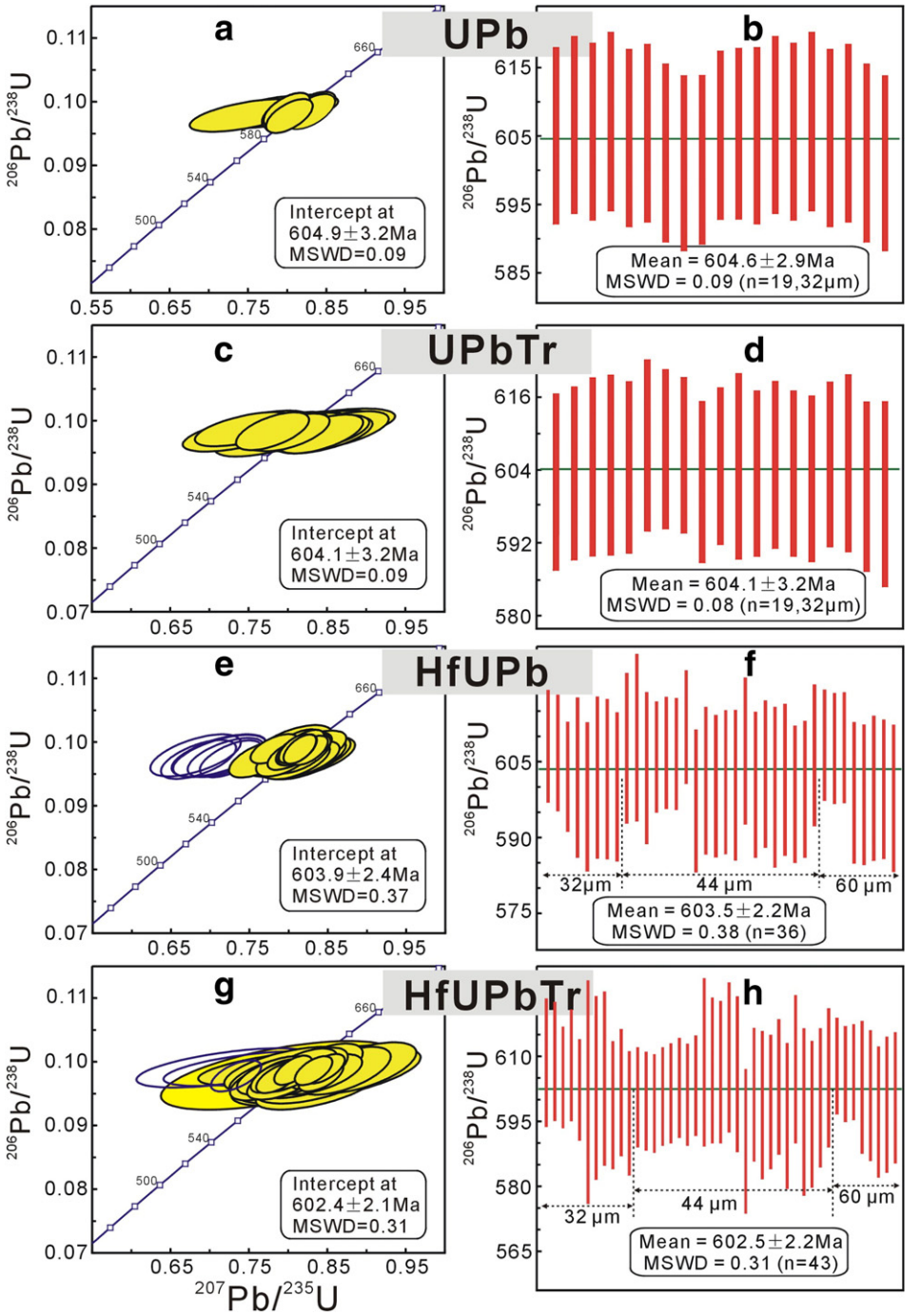

Fig. 7. U–Pb concordia diagrams showing the results obtained for zircon GJ-1 measured using (a) the UPb method, (c) the UPbTr method, (e) the HfUPb method, and (g) the HfUPbTr method. Corresponding distributions of the weighted average $^{206}Pb/^{238}U$ ages are shown in (b), (d), (f), and (h), respectively. Uncertainties are 2σ. The blank points in (e) and (g) are ablated on a 32 μm spot size.

$^{206}Pb/^{238}U$ and $^{207}Pb/^{206}Pb$ ages for this standard are 559.0±0.3 Ma (2σ, MSWD=0.86) and 562.2±0.5 Ma (2σ, MSWD=0.15), respectively (Stern, 2001). The U–Pb ages measured using the UPb, UPbTr, HfUPb, and HfUPbTr methods are shown in Fig. 8a–h. The weighted average $^{206}Pb/^{238}U$ ages are 560.5±1.9 Ma (2σ, MSWD=0.08, n=21, spot size=32 μm; Fig. 8b), 560.2±2.3 Ma (2σ, MSWD=0.08, n=21, spot size=32 μm; Fig. 8d), 559.3±2.3 Ma (2σ, MSWD=0.43, n=21, 32, 44, and 60 μm; Fig. 8f), and 561.0±2.2 Ma (2σ,

MSWD=0.10, n=29, spot size=32, 44, and 60 μm; Fig. 8h), respectively. All of these ages agree well with the ID-TIMS results within 2σ error.

Fig. 4d shows the chondrite-normalized REE patterns obtained from 21 analyses conducted employing the UPbTr and HfUPbTr methods. The results demonstrate that the REE compositions of this zircon are the most homogeneous of the six analyzed standards. The total REE contents of BR266 vary by <33%, which is significantly less than that within zircon 91500 (<100%;

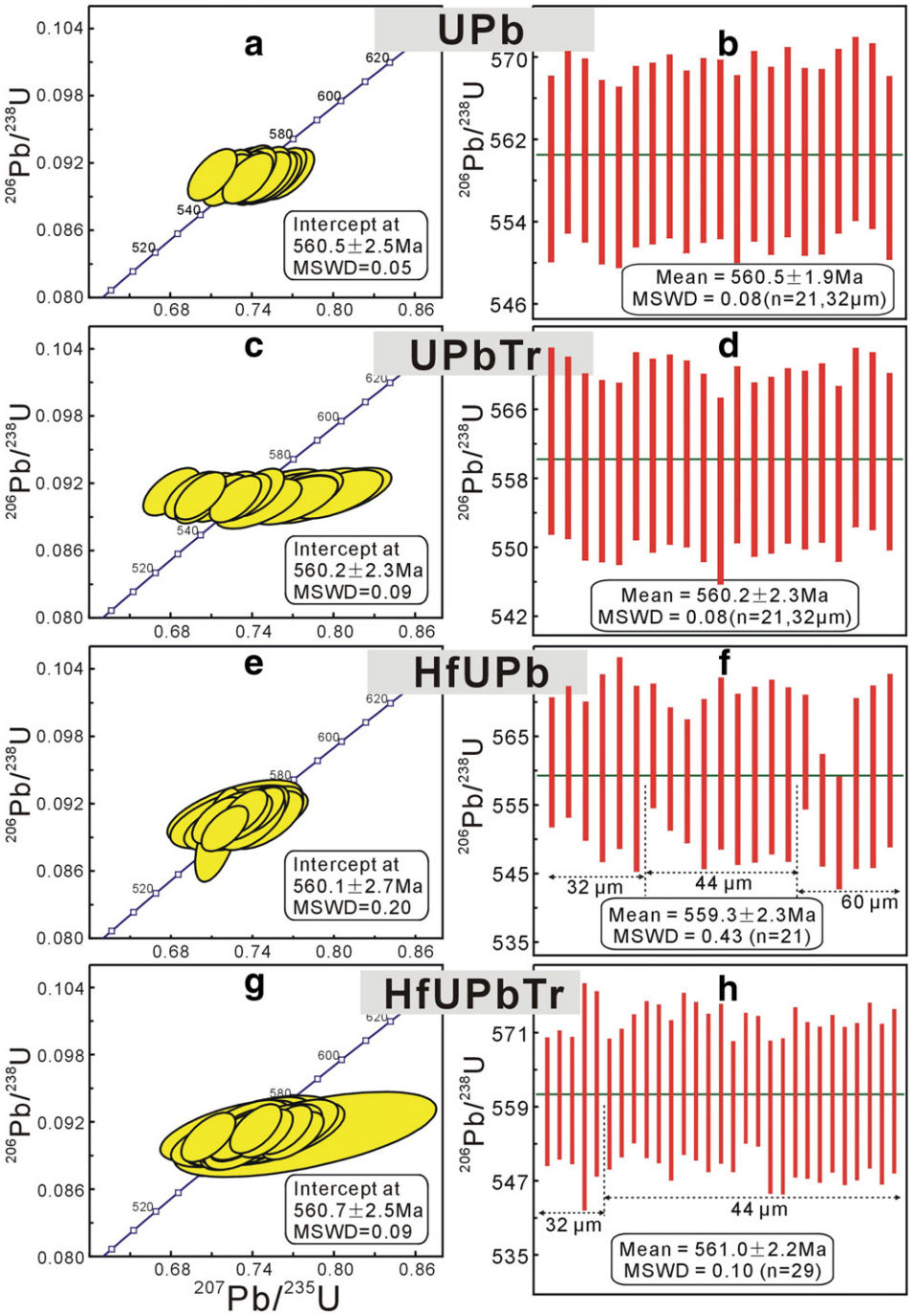

Fig. 8. U–Pb concordia diagrams showing the results obtained for zircon BR266 measured using (a) the UPb method, (c) the UPbTr method, (e) the HfUPb method, and (g) the HfUPbTr method. Corresponding distributions of the weighted average $^{206}Pb/^{238}U$ ages are shown in (b), (d), (f), and (h), respectively. Uncertainties are 2σ.

Yuan et al., 2004), Temora-2 (<464%), GJ-1 (<43%), Mud Tank (<122%), and Monastery (<84%) (Supplementary Table 2). Analysis of BR266 solution by MC-ICP-MS yielded a $^{176}Hf/^{177}Hf$ value of 0.281630±0.000010 (2σ), while long-term LA-MC-ICP-MS measurements averaged 0.281621±0.000024 (Woodhead et al., 2004; Woodhead and Hergt, 2005). For spot sizes of 32, 44, and 60 μm, the HfUPb and HfUPbTr methods yield weighted average $^{176}Hf/^{177}Hf$ ratios of 0.281620±0.000013 (2σ, MSWD=1.16, n=15), 0.281616±0.000005 (2σ, MSWD=0.85, n=28), and 0.281611±0.000009 (2σ, MSWD=0.98, n=6), respectively. The overall weighted average is 0.281616±0.000004 (2σ, MSWD=0.95, n=49; Fig. 9a), and the Hf method yields a weighted average $^{176}Hf/^{177}Hf$ value of 0.281621±0.000004 (2σ, MSWD=4.6, n=32, spot size=44 μm; Fig. 9b). These values agree with the recommended values within 2σ error. The high degree of homogeneity in terms of hafnium isotopic compositions, U–Pb age, and REEs demonstrates that this standard is well-suited for the evaluation of new external standards for microprobe analysis.

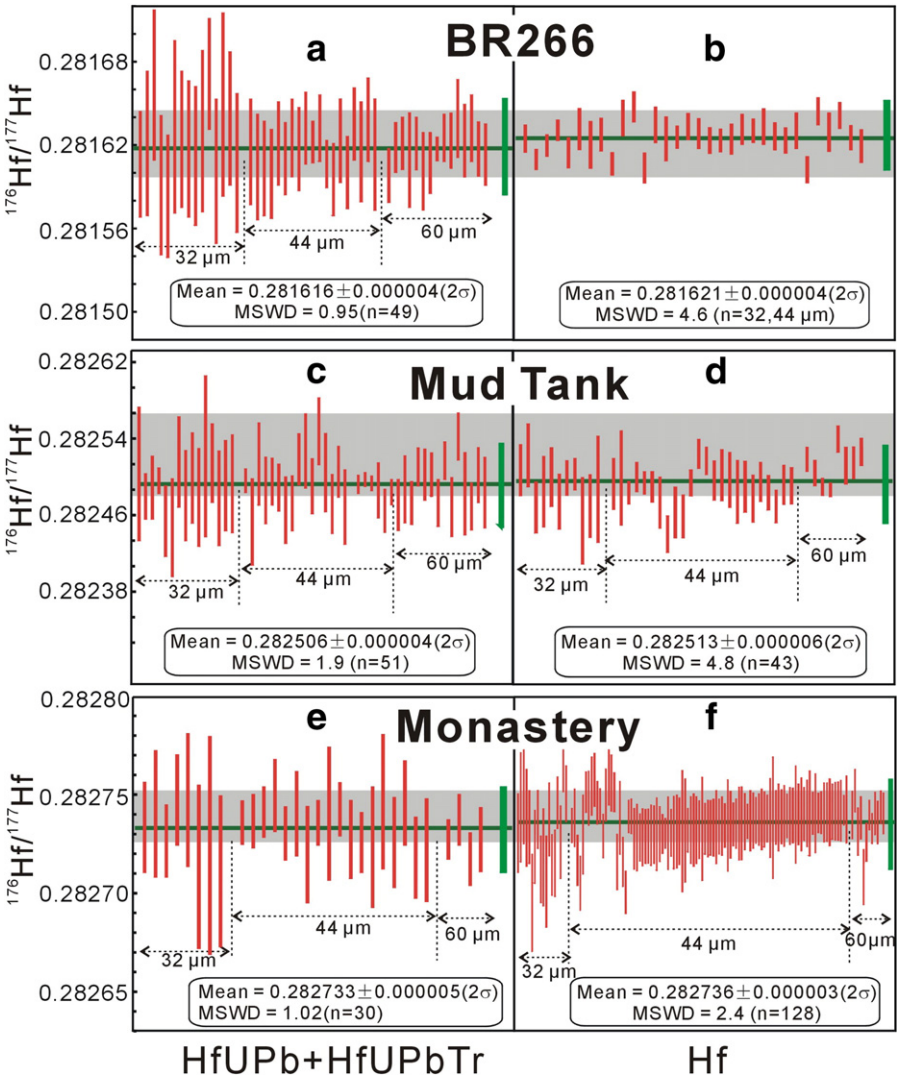

Fig. 9. $^{176}Hf/^{177}Hf$ ratios obtained for the zircon standards BR266, Mud Tank, and Monastery. The thick horizontal line and grey area in each panel represent the weighted average $^{176}Hf/^{177}Hf$ ratios determined in the present study and the 2σ error of the recommended values (Woodhead and Hergt, 2005), respectively. The thick vertical bar on the right side of each panel represents the 2σ range of the overall weighted average of analyses for spot sizes of 32, 44, and 60 μm.

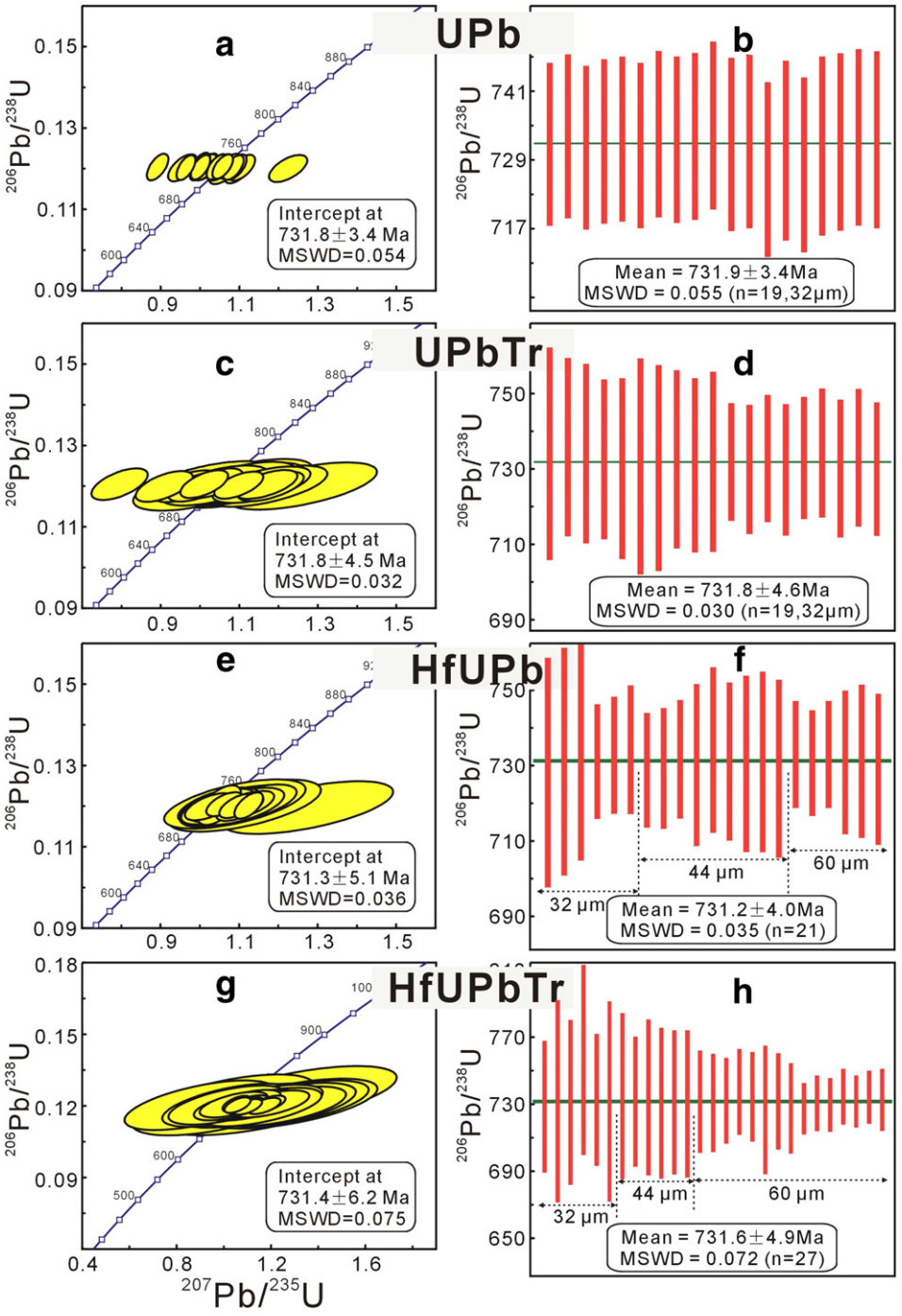

Fig. 10. U–Pb concordia diagrams showing the results obtained for the zircon Mud Tank measured using (a) the UPb method, (c) the UPbTr method, (e) the HfUPb method, and (g) the HfUPbTr method. Corresponding distributions of the weighted average $^{206}Pb/^{238}U$ ages are shown in (b), (d), (f), and (h), respectively. Uncertainties are 2σ.

4.5. Mud Tank

The Mud Tank Carbonatite occurs in the Strangways Range of the Northern Territory of Australia, ~150 km northeast of Alice Springs (Black and Gulson, 1978; Currie et al., 1992). The reported ID-TIMS age of zircons from this carbonatite is 732±5 Ma (Black and Gulson, 1978). The weighted average $^{206}Pb/^{238}U$ ages obtained using the

UPb, UPbTr, HfUPb, and HfUPbTr methods in the present study are 731.9±3.4 Ma (2σ, MSWD=0.055, n=19, spot size=32 μm; Fig. 10b), 731.8±4.6 Ma (2σ, MSWD=0.030, n=19, spot size=32 μm; Fig. 10d), 731.2±4.0 Ma (2σ, MSWD=0.035, n=21, spot size=32, 44, and 60 μm; Fig. 10f), and 731.6±4.9 Ma (2σ, MSWD=0.072, n=27, spot size=32, 44, and 60 μm; Fig. 10h), respectively.

REE concentrations determined using the HfUPbTr method on a spot size of 44 μm overlap with those measured using the UPbTr method on a spot size of 32 μm (Fig. 4e); however, HfUPbTr yielded lower concentrations than the UPbTr method.

The Hf isotopic composition of this standard has been well-characterized by Woodhead and Hergt (2005). These authors showed that although this gem-quality zircon exhibits strong zonation under cathodoluminescence and its Yb signal and Lu/Hf ratio vary systematically with zoning, its hafnium concentration and hafnium isotopic composition show negligible variation. On this basis, the authors concluded that Mud Tank is a robust reference material.

Weighted average $^{176}Hf/^{177}Hf$ ratios of both colorless and colored Mud Tank zircons, based on long-term extensive LA-MC-ICP-MS analyses, are 0.282523±0.000043 (2σ, n=2190; Griffin et al., 2006) and 0.282504±0.000044 (2σ, n=158; Woodhead and Hergt, 2005), respectively, whereas solution MC-ICP-MS measurements after chemical separation yield a value of 0.282507±0.000006 (2σ, n=5; Woodhead and Hergt, 2005). For spot sizes of 32, 44, and 60 μm, the Hf method yields weighted average $^{176}Hf/^{177}Hf$ ratios of 0.282511±0.000008 (2σ, MSWD=1.7, n=11), 0.282507±0.000006 (2σ, MSWD=1.9, n=24), and 0.282520±0.000016 (2σ, MSWD=11.0, n=8), respectively. The overall average of these spot sizes is 0.282513±0.000006 (2σ, MSWD=4.8, n=43; Fig. 9d). In comparison, the HfUPb and HfUPbTr methods together yield values of 0.282503±0.000008 (2σ, MSWD=0.88, n=15), 0.282504±0.000007 (2σ, MSWD=1.4, n=15), and 0.282507±0.000007 (2σ, MSWD=3.1, n=21) for spot sizes of 32, 44, and 60 μm, respectively. These values yield an overall weighted average of 0.282506±0.000004 (2σ, MSWD=1.9, n=51; Fig. 9c), which is only slightly lower than the overall average determined using the Hf method alone. All of these results agree with the recommended value within 2σ error.

4.6. Monastery

The Monastery megacryst zircon is derived from a 90 Ma Group I kimberlite pipe located in the southeast part of Free State, South Africa (Gurney et al., 1979). The zircon contains very low U–Pb concentrations [U<13 parts per million (ppm); Pb<3 ppm; Supplementary Table 1], making it unsuitable as a standard for U–Pb dating. Our 34 measurements of this zircon using the UPb, UPbTr, HfUPb, and HfUPbTr methods yield a $^{206}Pb/^{238}U$ age of 101.9±2.2 (2σ, MSWD=2.2, n=34; Supplementary Table 1). Griffin et al. (2000) reported that the $^{176}Hf/^{177}Hf$ ratios for this zircon range from 0.282661±0.000020 (2σ) to 0.282740±0.000015 (2σ), with an average of 0.282703±0.000030 (2σ, n=42); their 42 analyses show a unimodal distribution. However, subsequent evaluations by Woodhead and Hergt (2005) yielded ratios of 0.282738±0.000004 (2σ) using solution MC-ICP-MS and 0.282739±0.000013 (2σ, n=83) using LA-MC-ICP-MS.

For spot sizes of 32, 44, and 60 μm, our Hf method yields weighted average $^{176}Hf/^{177}Hf$ ratios of 0.282733±0.000012 (2σ, MSWD=4.3, n=18), 0.282736±0.000003 (2σ, MSWD=2.0, n=98), and 0.282737±0.000008 (2σ, MSWD=3.3, n=12), respectively. The overall average for these spot sizes is 0.282736±0.000003 (2σ, MSWD=2.4, n=128; Fig. 9f). The HfUPb and HfUPbTr methods yield 0.282733±0.000013 (2σ, MSWD=0.75, n=8) and 0.282736±0.000006 (2σ, MSWD=0.91, n=18) for spot sizes of 32 and 44 μm, respectively, giving an overall weighted average of 0.282733±0.000005 (2σ, MSWD=1.02, n=30, spot size=32, 44, and 60 μm; Fig. 9e). Our results agree with those reported by Woodhead and Hergt (2005), and are within the range determined by Griffin et al. (2000). The REE concentrations measured using the HfUPbTr method agree with those acquired using the UPbTr method (Fig. 4f).

Because this zircon contains extremely low Yb and Lu concentrations ($^{176}Yb/^{177}Hf$ and $^{176}Lu/^{177}Hf$ ratios of <0.001 and <0.00002, respectively) and relatively homogeneous Hf isotopic compositions, it is well-suited for monitoring instrumental drift during Hf isotope analyses in real samples.

5. Conclusions

We developed accurate *in situ* methods for the simultaneous measurement of U–Pb–Hf isotope and trace element compositions on the same spot (44 μm) within zircon. Our obtained U–Pb ages and Hf isotopic compositions for six standard zircons agree within 2σ error with recommended or existing values reported in previous studies, thereby demonstrating the feasibility of the proposed methods. The REE composition of zircon BR266 is relatively homogeneous, making it is an ideal standard for evaluating new standards for microprobe analyses of

zircons. Our methods provide a precise approach to measurements of the U–Pb age and Hf isotopic and trace element compositions of zircon for a single ablation event; such an approach is critical in some zircon studies, especially those dealing with small zircons and zircons with complicated zoning. Our methods are also potentially useful in any applications that require trace element concentrations and isotopic compositions determined from a single sampling site.

Acknowledgments

This work was supported by the National Nature Science Foundation of China (Grants 40521001, 40672029, 40302015 and 40673019), the Ministry of Education of China (Grants IRT0441, 306021 and B07039), and the National Basic Research Program of China (2003CA214600) to S. Gao and H.L. Yuan. We thank Carl Francis, Lance Black, Allen Kennedy, Steve Wilson, Uwe Wiechert, Jon Woodhead and Richard A. Stern for providing the standard zircons, John C. Ayers for polishing English, and Jinli Zhang for help in figure preparation. We also thank T. Hirata and Jon Woodhead for constructive comments which help to improve the manuscript significantly. We finally thank R.L. Rudnick for handling.

Appendix A. Supplementary data

Supplementary data associated with this article can be found, in the online version, at doi:10.1016/j.chemgeo.2007.10.003.

References

Albarède, F., Telouk, P., Blichert-Toft, J., Boyet, M., Agranier, A., Nelson, B., 2004. Precise and accurate isotopic measurements using multiple-collector ICPMS. Geochim. Cosmochim. Acta 68, 2725–2744.

Andersen, T., Griffin, W.L., Pearson, N.J., 2002. Crustal evolution in the SW part of the Baltic Shield: the Hf isotope evidence. J. Petrol. 43, 1725–1747.

Ballard, J.R., Palin, J.M., Williams, I.S., Campbell, I.H., Faunes, A., 2001. Two ages of porphyry intrusion resolved for the super-giant Chuquicamata copper deposit of northern Chile by ELA-ICP-MS and SHRIMP. Geology 29, 383–386.

Belousova, E.A., Griffin, W.L., O'Reilly, S.Y., Fisher, N.I., 2002. Igneous zircon: trace element composition as an indicator of source rock type. Contrib. Mineral. Petrol. 143, 602–622.

Belshaw, N.S., Freedman, P.A., O'Nions, R.K., Frank, M., Guo, Y., 1998. A new variable dispersion double-focusing plasma mass spectrometer with performance illustrated for Pb isotopes. Int. J. Mass Spectrom. 181, 51–58.

Black, L.P., Gulson, B.L., 1978. The age of the Mud Tank carbonatite, Strangways Range, Northern Territory. BMR J. Aust. Geol. Geophys. 3, 227–232.

Black, L.P., Kamo, S.L., Allen, C.M., Davis, D.W., Aleinikoff, J.N., Valley, J.W., Mundil, R., Campbell, I.H., Korsch, R.J., Williams, I.S., Foudoulis, C., 2004. Improved $^{206}Pb/^{238}U$ microprobe geochronology by the monitoring of a trace-element-related matrix effect; SHRIMP, ID-TIMS, ELA-ICP-MS and oxygen isotope documentation for a series of zircon standards. Chem. Geol. 205, 115–140.

Blichert-Toft, J., Albarède, F., 1997. The Lu–Hf isotope geochemistry of chondrites and the evolution of the mantle–crust system. Earth Planet. Sci. Lett. 148, 243–258.

Blichert-Toft, J., Albarède, F., Kornprobst, J., 1999. Lu–Hf isotope systematics of garnet pyroxenites from Beni Bousera, Morocco: implications for basalt origin. Science 283, 1303–1306.

Chu, N.C., Taylor, R.N., Chavagnac, V., Nesbitt, R.W., Boella, R.M., Milton, J.A., German, C.R., Bayon, G., Burton, K., 2002. Hf isotope ratio analysis using multi-collector inductively coupled plasma mass spectrometry: an evaluation of isobaric interference corrections. J. Anal. At. Spectrom. 17, 1567–1574.

Currie, K.L., Knutson, J., Temby, P.A., 1992. The Mud Tank carbonatite complex, central Australia—an example of metasomatism at mid-crustal levels. Contrib. Mineral. Petrol. 109, 326–339.

Eggins, S.M., Kinsley, L.P.J., Shelley, J.M.M., 1998. Deposition and elemental fractionation processes during atmospheric pressure laser sampling for analysis by ICP-MS. Appl. Surf. Sci. 127/129, 278–286.

Elhlou, S., Belousova, E., Griffin, W.L., Pearson, N.J., O'reilly, S.Y., 2006. Trace element and isotopic composition of GJ red zircon standard by laser ablation. Geochim. Cosmochim. Acta 70, A158. doi:10.1016/j.gca.2006.06.1383 (Supplement 1).

Gao, S., Liu, X.M., Yuan, H.L., Hattendorf, B., Günther, D., Chen, L., Hu, S.H., 2002. Determination of forty two major and trace elements in USGS and NIST SRM glasses by laser ablation-inductively coupled plasma-mass spectrometry. Geostand. Newsl. 26, 181–195.

Griffin, W.L., Pearson, N.J., Belousova, E., Jackson, S.E., van Achterbergh, E., Suzanne, Y.O., Shee, S.R., 2000. The Hf isotope composition of cratonic mantle: LAM-MC-ICPMS analysis of zircon megacrysts in kimberlites. Geochim. Cosmochim. Acta 64, 133–147.

Griffin, W.L., Wang, X., Jackson, S.E., Pearson, N.J., O'Reilly, S.Y., Xu, X., Zhou, X., 2002. Zircon chemistry and magma mixing, SE China: *in-situ* analysis of Hf isotopes, Tonglu and Pingtan igneous complexes. Lithos 61, 237–269.

Griffin, W.L., Belousova, E.A., Shee, S.R., Pearson, N.J., O'Reilly, 2004. Archaean crustal evolution in the northern Yilgarn Craton: U–Pb and Hf-isotope evidence from detrital zircons. Precambrian Res. 131, 231–282.

Griffin, W.L., Pearson, N.J., Belousova, E.A., Saeed, A., 2006. Comment: Hf-isotope heterogeneity in zircon 91500. Chem. Geol. 233, 358–363.

Guillong, M., Horn, I., Günther, D., 2003. A comparison of 266 nm, 213 nm and 193 nm produced from a single solid state Nd:YAG laser for laser ablation ICP-MS. J. Anal. At. Spectrom. 18, 1224–1230.

Günther, D., Heinrich, C.A., 1999a. Comparison of the ablation behaviour of 266 nm Nd:YAG and 193 nm ArF excimer lasers for LA-ICP-MS analysis. J. Anal. At. Spectrom. 14, 1369–1374.

Günther, D., Heinrich, C.A., 1999b. Enhanced sensitivity in laser ablation-ICP mass spectrometry using helium–argon mixtures as aerosol carrier. J. Anal. At. Spectrom. 14, 1363–1368.

Gurney, J.J., Jacob, W.R., Dawson, J.B., 1979. Megacrysts from the Monastery kimberlite pipe, South Africa. In: Boyd, R.R., Meyer, H.O.A. (Eds.), Kimberlites, Diatremes and Diamonds: Their Geology, Petrology and Geochemistry. American Geophysical Union, Washington, DC, pp. 222–243.

Halliday, A.N., Lee, D.C., Christensen, J.N., Rehkamper, M., Yi, W., Luo, X.Z., Hall, C.M., Ballentine, C.J., Pettke, T., Stirling, C., 1998. Applications of multiple collector-ICPMS to cosmochemistry,

geochemistry, and paleoceanography. Geochim. Cosmochim. Acta 62, 919–940.
Harrison, T.M., Blichert-Toft, J., Muller, W., Albarede, F., Holden, P., Mojzsis, S.J., 2005. Heterogeneous Hadean hafnium: evidence of continental crust at 4.4 to 4.5 Ga. Science 310, 1947–1950.
Hawkesworth, C.J., Kemp, A.I.S., 2006a. Evolution of the continental crust. Nature 443. doi:10.1038/nature05191.
Hawkesworth, C.J., Kemp, A.I.S., 2006b. Using hafnium and oxygen isotopes in zircons to unravel the record of crustal evolution. Chem. Geol. 226. doi:10.1016/j.chemgeo.2005.09.018.
Hirata, T., Nesbitt, R.W., 1995. U–Pb isotope geochronology of zircon: evaluation of the laser probe-inductively coupled plasma mass spectrometry technique. Geochim. Cosmochim. Acta 59, 2491–2500.
Hirata, T., Iizuka, T., Orihashi, Y., 2005. Reduction of mercury background on ICP-mass spectrometry for *in situ* U–Pb age determinations of zircon samples. J. Anal. At. Spectrom. 20. doi:10.1039/b504153h.
Horn, I., Rudnick, R.L., McDonough, W.F., 2000. Precise elemental and isotope ratio determination by simultaneous solution nebulization and laser ablation-ICP-MS: application to U–Pb geochronology. Chem. Geol. 167, 405–425.
Hoskin, P.W.O., Schaltegger, U., 2003. In: Hanchar, J.M., Hoskin, P.W.O. (Eds.), The Composition of Zircon and Igneous and Metamorphic Petrogenesis. Zircon. Rev. Mineral. Geochem., vol. 53, pp. 27–62.
Iizuka, T., Hirata, T., 2004. Simultaneous determinations of U–Pb age and REE abundances for zircons using ArF excimer laser ablation-ICPMS. Geochem. J. 38, 229–241.
Iizuka, T., Hirata, T., 2005. Improvements of precision and accuracy in *in situ* Hf isotope microanalysis of zircon using the laser ablation-MC-ICPMS technique. Chem. Geol. 220, 121–137.
Jackson, S.E., Pearson, N.J., Griffin, W.L., Belousova, E.A., 2004. The application of laser ablation-inductively coupled plasma-mass spectrometry to *in situ* U–Pb zircon geochronology. Chem. Geol. 211, 47–69.
Kamenov, G.D., Mueller, P.A., Perfit, M.R., 2004. Optimization of mixed Pb–Tl solutions for high precision isotopic analyses by MC-ICP-MS. J. Anal. At. Spectrom. 19, 1262–1267.
Kinny, P.D., Maas, R., 2003. In: Hanchar, J.M., Hoskin, P.W.O. (Eds.), Lu–Hf and Sm–Nd Isotope Systems in Zircon. Zircon. Rev. Mineral. Geochem., vol. 53, pp. 327–341.
Košler, J., Fonneland, H., Sylvester, P., Tubrett, M., Pedersen, R.B., 2002. U–Pb dating of detrital zircons for sediment provenance studies—a comparison of laser ablation ICPMS and SIMS techniques. Chem. Geol. 182, 605–618.
Li, X.H., Liang, X.R., Sun, M., Liu, Y., Tu, X., 2000. Geochronology and geochemistry of single–grain zircons: simultaneously in–situ analysis of U–Pb age and trace elements by LAM–ICP–MS. Eur. J. Mineral. 12, 1015–1024.
Li, X.H., Liang, X.R., Sun, M., Guan, H., Malpas, J.G., 2001. Precise ^{206}Pb–^{238}U age determination on zircons by laser ablation microprobe-inductively coupled plasma-mass spectrometry using continuous linear ablation. Chem. Geol. 175, 209–219.
Longerich, H.P., Fryer, B.J., Strong, D.F., 1987. Determination of lead isotope ratios by inductively coupled plasma-mass spectrometry (ICP-MS). Spectrochim. Acta, Part B: Atom. Spectrosc. 42, 39–48.
Ludwig, K.R., 2003. User's Manual for Isoplot 3.0: A Geochronological Toolkit for Microsoft Excel Berkeley Geochronology Center. special publication, vol. 4, pp. 1–71.
Maréchal, C.N., Télouk, P., Albarède, F., 1999. Precise analysis of copper and zinc isotopic compositions by plasma-source mass spectrometry. Chem. Geol. 156, 251–273.
Patchett, P.J., Kuovo, O., Hedge, C.E., Tatsumoto, M., 1981. Evolution of the continental crust and mantle heterogeneity: evidence from hafnium isotopes. Contrib. Mineral. Petrol. 78, 279–297.
Paul, B., Woodhead, J.D., Hergt, J., 2005. Improved *in situ* isotope analysis of low-Pb materials using LA-MC-ICP-MS with parallel ion counter and Faraday detection. J. Anal. At. Spectrom. 20, 1350–1357.
Pearce, N.J.G., Perkins, W.T., Westgate, J.A., Gorton, M.P., Jackson, S.E., Neal, C.R., Chenery, S.P., 1997. A compilation of new and published major and trace element data for NIST SRM 610 and NIST SRM 612 glass reference materials. Geostand. Newsl. 21, 115–141.
Qi, C.S., Li, X.H., Liang, X.R., Liu, Y., Tu, X.L., 2005. High-precision measurement of Hf isotopic reference values for the U–Pb geochronology standard zircons by multi-collector ICP-MS. J. Chin. Mass Spectrom. Soc. 26, 149–154 (in Chinese with English abstract).
Simonetti, A., Heaman, L.M., Hartlaub, R.P., Creaser, R.A., MacHattie, T.G., Böhm, C., 2005. U–Pb zircon dating by laser ablation-MC-ICP-MS using a new multiple ion counting Faraday collector array. J. Anal. At. Spectrom. 20, 677–686.
Stern, R.A., 2001. A new isotopic and trace-element standard for the ion microprobe: preliminary thermal ionisation mass spectrometry (TIMS) U–Pb and electron-microprobe data. Radiogenic Age and Isotope Studies, Report 14, Geological Survey of Canada, Current Research, 2001-F.
Storey, C.D., Jeffries, T.E., Smith, M., 2006. Common lead-corrected laser ablation ICP-MS U–Pb systematics and geochronology of titanite. Chem. Geol. 227. doi:10.1016/j.chemgeo.2005.09.003.
Taylor, S.R., McLennan, S.M., 1985. The Continental Crust: Its Composition and Evolution. Blackwell, Oxford, pp. 1–312.
Vance, D., Thirlwall, M., 2002. An assessment of mass discrimination in MC-ICPMS using Nd isotopes. Chem. Geol. 185, 227–240.
Vervoort, J.D., Patchett, P.J., Söderlund, U., Baker, M., 2004. Isotopic composition of Yb and the determination of Lu concentrations and Lu/Hf ratios by isotope dilution using MC-ICPMS. Geochem. Geophys. Geosyst. 5. doi:10.1029/2004GC000721.
Walder, A.J., Koller, D., Reed, N.M., Hutton, R.C., Freedman, P.A., 1993. Isotope ratio measurements by inductively coupled plasma-multiple collector-mass spectrometry incorporating a high efficiency nebulization system. J. Anal. At. Spectrom. 8, 1037–1041.
Watson, E.B., Harrison, T.M., 2005. Zircon thermometer reveals minimum melting conditions on earlier earth. Science 308, 841–844.
Watson, E.B., Wark, D.A., Thomas, J.B., 2006. Crystallization thermometers for zircon and rutile. Contrib. Mineral. Petrol. 151, 413–433.
Whitehouse, M.J., 2004. Multi-collector SIMS determination of trace lanthanides in zircon. Geostand. Geoanal. Res. 28, 195–201.
Wiedenbeck, M., Alle, P., Corfu, F., Griffin, W.L., Meier, M., Oberli, F., Vonquadt, A., Roddick, J.C., Speigel, W., 1995. Three natural zircon standards for U–Th–Pb, Lu–Hf, trace-element and REE analyses. Geostand. Newsl. 19, 1–23.
Wiedenbeck, M., Hanchar, J.M., Peck, W.H., Sylvester, P., Valley, J., Whitehouse, M., Kronz, A., Morishita, Y., Nasdala, L., Fiebig, J., Franchi, I., Girard, J.P., Greenwood, R.C., Hinton, R., Kita, N., Mason, P.R.D., Norman, M., Ogasawara, M., Piccoli, R., Rhede, D., Satoh, H., Schulz-Dobrick, B., Skar, O., Spicuzza, M.J., Terada, K., Tindle, A., Togashi, S., Vennemann, T., Xie, Q., Zheng, Y.F., 2004. Further characterisation of the 91500 zircon crystal. Geostand. Geoanal. Res. 28, 9–39.
Woodhead, J.D., Hergt, J.M., 2005. Preliminary appraisal of seven natural zircon reference materials for *in situ* Hf isotope determination. Geostand. Geoanal. Res. 29, 183–195.
Woodhead, J., Hergt, J., Shelley, M., Eggins, S., Kemp, R., 2004. Zircon Hf-isotope analysis with an excimer laser, depth profiling,

ablation of complex geometries, and concomitant age estimation. Chem. Geol. 209, 121–135.

Wu, F.Y., Yang, Y.H., Xie, L.W., Yang, J.H., Xu, P., 2006a. Hf isotopic compositions of the standard zircons and baddeleyites used in U–Pb geochronology. Chem. Geol. 232. doi:10.1016/j.chemgeo.2006.05.003.

Wu, Y.B., Zheng, Y.F., Zhao, Z.F., Gong, B., Liu, X., Wu, F.Y., 2006b. U–Pb, Hf and O isotope evidence for two episodes of fluid-assisted zircon growth in marble-hosted eclogites from the Dabie orogen. Geochim. Cosmochim. Acta 70, 3743–3761.

Xu, P., Wu, F.Y., Xie, L.W., Yang, Y.H., 2004. Hf isotopic compositions of the standard zircons for U–Pb dating. Chin. Sci. Bull. 49, 1642–1648.

Yuan, H.L., Gao, S., Liu, X.M., Li, H.M., Günther, D., Wu, F.Y., 2004. Accurate U–Pb age and trace element determinations of zircon by laser ablation inductively coupled plasma-mass spectrometry. Geostand. Geoanal. Res. 28, 353–370.

Zheng, Y.F., Wu, Y.B., Zhao, Z.F., Zhang, S.B., Xu, P., Wu, F.Y., 2005. Metamorphic effect on zircon Lu–Hf and U–Pb isotope systems in ultrahigh-pressure eclogite-facies metagranite and metabasite. Earth Planet. Sci. Lett. 240, 378–400.